Microphase Separation in Polymer + Surfactant Systems†

B. Cabane,*,‡ K. Lindell,§ S. Engström,§ and B. Lindman⊥

Equipe mixte CEA-RP, Service de Chimie Moléculaire, CE-Saclay, 91191 Gif sur Yvette, France, and Departments of Food Technology and Physical Chemistry 1, Chemical Center, University of Lund, P.O.B. 124, S-221 00 Lund, Sweden

Received October 12, 1995; Revised Manuscript Received February 5, 1996⊗

ABSTRACT: Some cellulosic derivatives are soluble in cold water, but above a clouding temperature they form a polymer-rich phase which progressively expels water as the temperature is raised. This phase separation may be modified by adding surfactants. Over a certain range of compositions and temperatures, some of these systems form thermoreversible gels. Small angle neutron scattering experiments are reported for the gels made of ethyl hydroxyethyl cellulose (type CP-30) and cationic surfactants. The results show that the surfactants cause a dissociation of the polymer-rich phase into smaller lumps, with sizes on the order of 500 Å. Each lump is formed by the loose association of polymer strands belonging to many macromolecules and is covered by surfactant. The mechanical rigidity of the gel originates from the association of the macromolecules through these lumps.

Introduction

In water, many soluble polymers exhibit *associative properties*.[1,2] These polymers are made of two types of monomers. Some monomers (type A) are hydrophilic; they cause the hydration and swelling of the polymer in the presence of water. Others (type B) are hydrophobic; they tend to reduce their hydration by associating together. This combination of *swelling* and *association* determines the thermodynamic states and the properties of the polymer in water. Depending on the strength of association, the thermodynamic states may be as follows

(i) states where the macromolecules are fully dissociated, i.e. true solutions.

(ii) states where the macromolecules bind to each other but nevertheless swell to occupy all the volume offered by the solvent, i.e. gels.

(iii) states where the binding causes the macromolecules to concentrate in a smaller volume and separate from excess water, i.e. precipitates.

A description of each state must be at two levels: connectivity and microstructure. *Connectivity* is defined by the paths through which remote strands are linked to each other; it is determined by the way in which sequences of B monomers bind to each other. *Structure* is defined by the spatial distributions of A and B; it results from the polymer's attempts to maximize A-W contacts (swelling) and minimize B-W contacts (B-B association). These attempts usually cause some kind of segregation of B from A.

The situation is easiest to understand with polymers that have regular sequences, e.g. *block copolymers*.[3] In this case the macromolecules can find configurations that minimize B−W contacts without limiting the hydration of A sequences (Figure 1). Increasing the strength of association causes the formation of periodic structures where the B monomers are located in spherical, cylindrical, or lamellar domains. These structures yield association (in domains) and connectivity (between domains); they may be controlled by changing the proportions of A or B monomers, the amount of water, and the lengths of blocks.

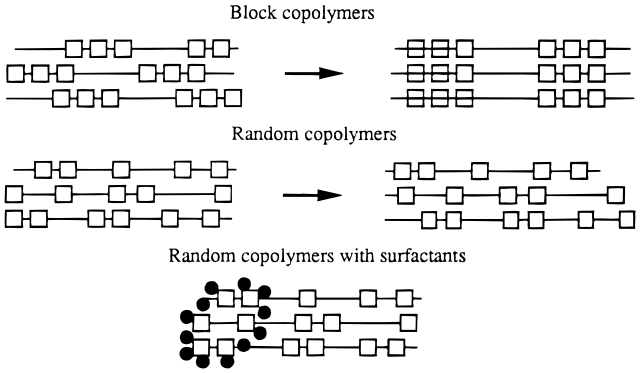

Figure 1. Pictures of segregation in block copolymers versus random copolymers.

A more difficult situation prevails with *random copolymers*. These macromolecules are unable to find configurations that achieve substantial dehydration of B monomers without losing the swelling of A sequences (or unable to swell A sequences without pulling B monomers into the aqueous medium). Thus, the separation of B from A + W is incomplete (Figure 1). Increasing the strength of B−B associations results in macroscopic phase separation into a polymer-rich phase (A + B, not much W) and a water-rich phase.

Thus, random copolymers generally do not form aqueous gels. In order to obtain extensive connectivity without losing swelling, it is necessary to modify the phase separation behavior. This may be done through chemical means, by increasing the block character of the sequences, or through physical means, by adding surfactant. In this paper we examine how added surfactants modify the phase separation behavior of a random-like copolymer.

It is instructive to first examine a well-known situation. The interactions of ionic surfactants with nonionic *homopolymers* in water have been extensively studied.[4] These interactions are comparatively weak; it was found that the surfactant forms micelles and that the polymer adsorbs on the micellar surfaces.[5] If the macromolecules are long enough, each one may bind many surfactant micelles in a sort of "necklace".[6,7] No gels have been found;[8] this implies that a micelle cannot be shared by two adsorbing macromolecules. This behavior can be derived from the following rules: (a) the hydrophobic chains of the surfactant molecules must self-assemble to minimize their contacts with water; (b) the polymers must remain in water.

† This work used the neutron beams of LLB in Saclay, France.
‡ Service de Chimie Moléculaire.
§ Department of Food Technology, University of Lund.
⊥ Department of Physical Chemistry 1, University of Lund.
⊗ Abstract published in *Advance ACS Abstracts,* March 15, 1996.

0024-9297/96/2229-3188$12.00/0

With random *copolymers*, the interaction is stronger because the hydrophobic B monomers may bind to hydrophobic surfactant chains. Experimentally, the systems may be found as solutions, gels, or precipitates.[9−11] The problem is to understand this behavior in terms of rules for association, considering that (a) the hydrophobic domains will be formed of surfactant molecules and B monomers and (b) these hydrophobic domains may be connected by polymer sequences that have remained in water.

In the following we report small angle neutron scattering (SANS) experiments on systems containing a nonionic cellulose derivative, ethyl hydroxyethyl cellulose (EHEC), and a cationic surfactant (an alkyl betainate, abbreviated TeBo). These systems are typical of the situations described just above, since they form solutions, gels, and precipitates. Moreover, they belong to a particularly interesting class of mixtures, i.e. those where interactions of the polymer with water may be varied according to temperature; thus, thermoreversible gels are formed.[10−13] This thermal gelation is rather general with respect to the ionic surfactant: one can use almost any surfactant, as long as it is ionic and has a sufficiently long hydrocarbon tail.

From the SANS results we determined the structures of the mixed polymer + surfactant systems, with emphasis on the situation where the surfactant dominates the scattering. The use of temperature variations has allowed us to compare the states of the same system with different strengths of the interactions. In particular, these structural determinations shed some light on the nature of the gel state.

Materials and Sample Preparation

Polymers. Ethyl hydroxyethyl cellulose (EHEC) is produced by the chemical substitution of cellulose with ethylene and ethylene oxide groups. Cellulose consists of β-D-glucose as the monomeric units, which are linearly linked through the carbons at positions 1 and 4 in the pyranose ring. There are three hydroxyl groups per anhydroglucose that can be substituted. The highest degree of substitution for ethyl groups is thus 3.0 per unit. This value could actually be exceeded for ethyl oxide, since alkylene oxides (e.g., EO) can form oligomeric side chains. It is important to keep in mind that the values are average numbers that do not reflect the variations in the homogeneity of susbtitution.

EHEC designated DVT 89017 was obtained from Akzo Nobel Surface Chemistry AB (Stenungsund, Sweden). The average substitution degree was, according to the manufacturer, 1.9 ethyl groups and 1.3 ethylene oxide groups per anhydroglucose unit. The viscosity average molar mass was 100 000 g/mol. The clouding temperature (CP) was 34 °C in 1% (w/w) aqueous solution. Dilute solutions were desalted and purified against Milli-Q water by an Ultrasette (Filtron) tangential flow device with a pore size of 10 kDa. The polymer was freeze-dried after dialysis.

Surfactant and Salt. The cationic alkyl betainate, tetradecyl(oxycarbonyl)-*N*,*N*,*N*-trimethylmethanaminium chloride (TeBo) (from Akzo Nobel) and the salt, timolol maleate (TM) (from Sigma) were used as received.

Sample Preparation. Stock solutions of EHEC were prepared by addition of D_2O during agitation at room temperature followed by continuous stirring in a cool room (+5 °C) for at least 48 h to ensure complete dissolution. The resulting clear solutions were stored in a refrigerator until use. These solutions were equilibrated at room temperature (20−22 °C) before sample preparation or dilution. Salt (TM) was dissolved in the EHEC solution. Calculated amounts of solid surfactant and EHEC + salt solution were weighed into glass tubes, sealed with Teflon-coated screw-caps, and thoroughly mixed with a Whirlimixer shaking machine. All samples were then equilibrated at room temperature for at least 24 h, or until no detectable change in the phase behavior could be observed.

Phase Studies

The system studied in this work was initially chosen for its ability to form thermoreversible gels. This property could have a potential for biomedical applications, for instance as a drug delivery system to the eye. The constraints for such applications are as follows. The system must be fluid and transparent at room temperature and become a transparent gel at temperatures about 35 °C. This requires polymer concentrations in the semidilute range, on the order of 1% for the type of EHEC used here. Moreover, the system must be studied in the presence of salt, first because the drug, timolol maleate, is a salt and second because the tears that wet the eye are at physiological ionic strength. In this work, all samples were made with timolol maleate as a salt, at a concentration of 0.25%. The presence of salt has the consequence of shifting the regions of gelation to higher surfactant concentrations. We found that studies performed in the ranges 0−3% EHEC, 0−3% TeBo gave samples that reproduced the behaviors previously described in the literature, i.e. clouding, thermoreversible gelation, the so-called "white-gel" formation, and macroscopic phase separation.[10−13]

Methods. Phase maps were obtained in the temperature range of 20−60 °C. The samples were equilibrated in a block thermostat (Grant BT3) for 1 h at each temperature before investigation and with an increase of not more than 5 deg per step. The phase behavior was studied by visual observation and the macroscopic fluidity was estimated to define regions with the thermogelling property. Most of the samples were checked several times, after differing storage times, to confirm equilibrium conditions and detect any hysteresis effects. We have used the notation "phase map", instead of phase diagram, to emphasize that we are dealing with multicomponent systems. The EHEC samples are believed to be rather heterogeneous with respect to molecular weight distribution as well as degree and position of substitution, and some of the maps presented in this work also differ from ordinary phase diagrams in the sense that we have locked the composition of some of the components and thus made them presentable as pseudo two-component systems.

Phase Behavior of EHEC in Water. EHEC belongs to a class of nonionic polymers with reduced solubility in water at elevated temperatures. The batch used in this study had a cloud point (CP) of 34 °C, visually taken as the temperature where samples begin to scatter visible light and thus are transformed from perfectly clear to bluish, turbid solutions by eye. At temperatures above the clouding temperature, aqueous solutions of EHEC will, if left to stand, separate to a white, more or less brittle polymer-rich phase and a water phase containing almost no polymer.

A phase map for the EHEC used in this study in D_2O is shown in Figure 2. The temperature and the polymer concentration are represented on the vertical and horizontal axes, respectively. The filled line is to be considered as a cloud-point curve or, more correctly, as the turbidity boundary, below which all samples are clear and consist of only one phase. Above this line the samples scatter visible light. The polymer concentration dependence of the CP is very low: samples prepared through direct mixing, in the range from 0.2 to 3% EHEC, had a cloud point of 34 °C; samples prepared through osmotic stress, in the range from 5 to 18%

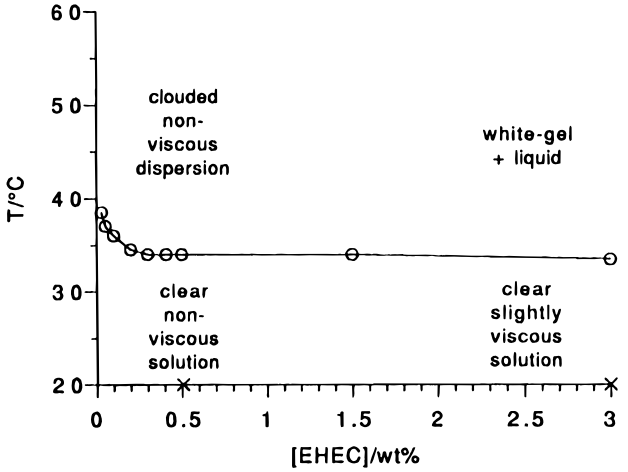

Figure 2. Phase diagram of EHEC, batch DVT 89017, in D_2O. This particular EHEC has been substituted with side groups to have a cloud point in the vicinity of 34 °C. Samples examined at temperatures below the phase separation line were one-phase, clear solutions. Samples examined at temperatures above the phase separation line were turbid dispersions (at low concentrations) or white gels that progressively expelled a transparent aqueous phase.

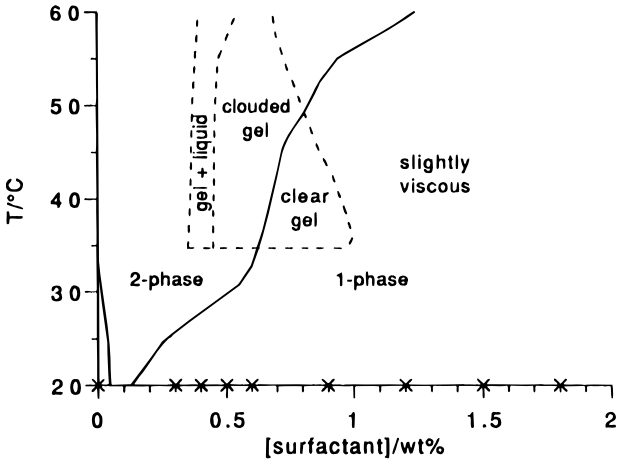

Figure 3. Phase map of mixed solutions containing a fixed polymer concentration (EHEC 1.5%), a fixed concentration of salt (TM 0.25%), and variable amounts of surfactant (TeBo). The continuous line marks the onset of turbidity or phase separation; the dotted lines refer to various types of gel formation.

EHEC, had the same cloud point at 34 °C. If the cloud point is taken as a LCST, then this LCST is remarkably flat.

At temperatures slightly above the cloud point, phase separation is observed. For instance, a 3% EHEC solution is clear and slightly viscous at room temperature; if it is kept at 40 °C, it first turns into a white gel and then later slowly separates into a dilute aqueous phase and a concentrated polymer phase; this is commonly referred to as a syneretical behavior. The EHEC concentration of the dilute aqueous phase is below 1%; the EHEC concentration of the polymer rich phase is of the order of 25%.

EHEC + TeBo + TM. In Figure 3, the corresponding phase map for a system including 1.5% EHEC DVT 89017, 0.25% timolol maleate (TM) and various amounts of the cationic surfactant alkyl betainate (TeBo) in D_2O is shown. The CP of the system without addition of surfactant is about 34 °C and seen as the intercept of the turbidity line with the temperature axis. This means that the presence of 0.25 wt % (5.8 mM) TM does not affect the behavior of the surfactant-free system. As

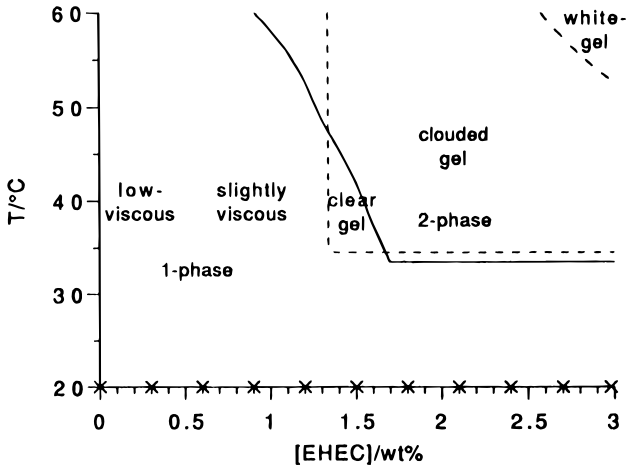

Figure 4. Phase map of mixed solutions containing a fixed surfactant concentration (TeBo 0.72%), a fixed concentration of salt (TM 0.25%), and variable amounts of polymer (EHEC).

the surfactant is added, the turbidity boundary is first seen to exhibit a minimum (in temperature) at low surfactant concentrations, which is then changed to a monotonical increase in CP with increasing amounts of surfactant. This shape of the curve is known to be a result of a synergistic effect of the simultaneous presence of salt (electrolytes) and ionic surfactant in the solution, which leads to a more or less pronounced minimum in CP as a function of surfactant concentration.[14]

The dotted lines indicate the domain where, with respect to the temperature and surfactant concentration, the most pronounced viscosity enhancement is found. This can further be divided into three parts depending on the visual appearance of the samples: "clear gels" formed below the turbidity line, "clouded gels" which are not macroscopically phase separated but scatter visible light, and "gel + liquid" where the gel coexists with a water-rich phase. The viscosity of samples outside but near the dotted area can also be substantially enhanced, indicating a gradual changeover, but the thermogelling property is then lost with increasing surfactant concentration and the samples at the far right become even less viscous than the polymer solution without surfactant at room temperature.

The phase map of a system with 0.25% TM, 0.72% TeBo, and various concentrations of EHEC DVT 89017 in D_2O is illustrated in Figure 4. Here are, as in the previous phase map, the filled line and the dotted area indicating the turbidity boundary and the domain exhibiting gel properties. This map could be regarded as an illustration of the gradual conversion from a system with a micellar solution of the ionic surfactant, from which the behavior is determined, to a system with 3% EHEC exhibiting properties rather like a surfactant-free concentrated polymer solution. The thermal gelation is starting to show up somewhere in the intermediate region, at about 1.3% polymer. The maps in Figures 3 and 4 are crossing at the points with 0.72% (20.6 mM) surfactant in Figure 3 and 1.50% EHEC in Figure 4.

Equilibrium State of the Samples. The phase maps show regions where the samples are turbid or opaque, mainly at elevated temperatures. The turbidity must result from heterogeneities of composition on a spatial scale comparable to the wavelength of light. Since some samples at the same temperatures show macroscopic phase separation, and others are not separated but opaque, these large scale homogeneities may

be described as incomplete phase separation. It is important to examine whether this incomplete separation is an equilibrium state of the sample or a transient state on the way to complete phase separation. This question may be answered by comparing the state of samples that have been brought to the same point in the phase map through different routes, e.g. heating or cooling.

For pure semidilute polymer solutions, fast heating does produce samples that have the appearance of white gels but phase separate at longer times. Similar observations have been made in most other aqueous solutions of cellulose derivatives. All these white gels are actually the first step to a macroscopic phase separation.

For polymer + surfactant solutions, we also observed slow phase separation in samples containing low amounts of surfactant. The region of phase separation is the gel + liquid region of the phase maps. In these samples, the expulsion of water by the gel took place over a few hours; at longer times the phase equilibrium remained the same, indicating that the gel phase is at osmotic equilibrium with the separating aqueous phase.

Compositions that gave clouded gels at 40 °C also expelled some water at higher temperatures. Upon cooling, this water was reabsorbed in the gel, indicating that the clouded gel could withstand cycles in temperature. Proof of equilibrium would require that the clouded gel would be destroyed at higher temperatures and re-formed upon cooling.

Compositions that gave transparent gels could be heated to give clouded gels, and cooled to give the transparent gel again. Therefore, the clear gels are an equilibrium state of the system.

These observations indicate that the equilibrium state is reached after a few hours in samples containing up to 3% EHEC. At higher concentrations, the approach to equilibrium takes much longer times, and homogeneous samples can be prepared only through osmotic stress.

Scattering Techniques

Contrasts. The small angle scattering of neutrons originates from the spatial variations in the sample of a quantity which acts as an index of refraction. This quantity is called the density of scattering length; it is calculated by summing in a small volume the scattering lengths of individual nuclei.[15,16] For aqueous solutions, what matters is how much the densities of scattering length of solutes differ from that of water. With organic solutes, the differences are usually small, unless isotopic subtitution of H by D is used. Replacing H_2O by D_2O or hydrogenated molecules by deuterated ones leads to large differences of scattering length.

In this work, we have used D_2O as a solvent. Consequently, the surfactants have a high contrast and cause a strong scattering. The case of the polymer is more subtle. Indeed, the alcohol protons may exchange with deuterons from water, thereby reducing the contrast of the polymer. In order to settle this point, we have measured the scattering of EHEC in different H_2O/D_2O mixtures and determined which mixture matches the density of scattering length of EHEC. We found that the scattering of EHEC vanishes in a mixture containing 76% H_2O and 24% D_2O. With this result we can compare the contrasts expected for EHEC and for the surfactant in D_2O. Because the intensities are proportional to the square of the differences in the density of scattering length, we can predict that the scattering of the surfactant will be, for equal amounts, 3 times larger than that of the polymer.

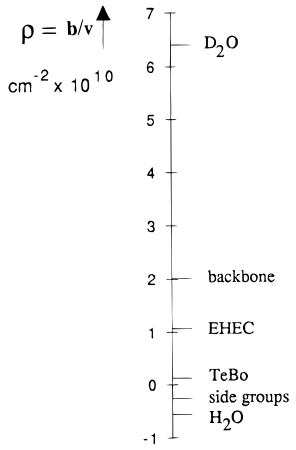

Figure 5. Scattering length densities of the components of the mixed solutions. The polymer backbone is matched by a 40/60 D_2O/H_2O mixture, and it has a low contrast in D_2O. The surfactant (TeBo) has a low contrast in H_2O and a high contrast in D_2O.

Alternatively, we may wish to compare the scattering from the hydrophobic components (surfactant chains and side groups of the polymer) with that from the hydrophilic components. All hydrophobic components carry a large number of nonexchangeable protons; therefore hydrocarbon chains and oxyethylene chains have a high contrast in D_2O. To the contrary, the sugars of the polymer backbone carry few nonexchangeable protons; therefore they will have a low contrast (Figure 5).

According to these calculations, we may assume that the hydrophobic components in the sample will produce most of the scattering when the samples are prepared in D_2O.

Scattering Curves. The scattering curves result from interferences between neutron rays scattered by different nuclei in the sample. The interferences are determined by the scalar product $\mathbf{Q}\cdot\mathbf{r}$, where $\mathbf{Q}$ is the scattering vector and $\mathbf{r}$ is the vector separating points. For isotropic samples, only the magnitude Q of the scattering vector matters, which is determined by the wavelength λ of incident neutrons and the scattering angle θ:

$$Q = (4\pi/\lambda)\sin(\theta/2) \tag{1}$$

Then the scattering pattern may be reduced to a scattering curve $I(Q)$. From this scattering curve, some geometrical parameters that characterize the distribution of scattering length in the sample may be determined. The description is easiest when the sample is a dispersion of identical, uncorrelated objects, because interferences between objects cancel out, and only interferences within each object need to be considered.

Dispersions of Identical, Uncorrelated Objects.[15,16] At $Q = 0$, all rays are in phase, and the scattered intensity measures the content of each object, as expressed by its volume V and its density of scattering length $\Delta\rho$:

$$I_0 = KNV^2(\Delta\rho)^2 \tag{2}$$

where K is an instrumental constant and N is the number of uncorrelated objects. Thus, the volume V per object or the corresponding mass can be extracted from the absolute value of I_0; alternatively, instead of determining the instrumental constant K, it is possible to

normalize I_0 by the integral of the intensity scattered in all directions.[16,19]

At low Q, the intensity decays because of interferences between rays scattered by points located at opposite ends of each object. The decay is related to the radius of gyration R_g of the object through the Guinier law:

$$I(Q\rightarrow 0) = I_0\,(1 - Q^2R_g{}^2/3) \qquad (3)$$

At intermediate Q values, the intensity decays faster, because all rays scattered by each object interfere destructively. The rate of the decay depends on the shape of the object: rodlike objects give a Q^{-1} decay, flat objects such as disks or shells give Q^{-2}, and dense globules follow Porod's law, which is Q^{-4}. The precise shape of the scattering curves may be calculated for objects that have a simple geometry. For homogeneous spheres of outer radius R, the scattering curve is a function that starts according to eq 3 and then oscillates around the Q^{-4} decay of Porod's law; the formula is

$$I_{\text{sphere}}(Q) = I_0[\sin QR - QR\cos QR]^2(QR)^{-6} \qquad (4)$$

For hollow shells, the general shape is similar, but the asymptotic decay is as Q^{-2}:

$$I_{\text{shell}}(Q) = I_0[(\sin QR_1 - QR_1\cos QR_1) - (\sin QR_2 - QR_2\cos QR_2)]^2(Q^3R_1{}^3 - Q^3R_2{}^3)^{-2} \qquad (5)$$

Dispersions of Nonidentical Objects. If the objects vary in their sizes, the intensity may be calculated by summing the contributions from each type of object. For spherical objects, this has the effect of smoothing out the oscillations of the scattering function, because the period of the oscillations is determined by the radius of the sphere. Similarly, if the objects are not spherical, the oscillations are also smoothed out, because the diameters observed in different directions are not the same.

In this work, we have used triangular distributions of spheres or shells. Similar fits would have been obtained with Gaussian distributions. The intensity was calculated as

$$I(Q) = K(\Delta\varrho)^2\sum[I_{\text{sphere}}(QR)] \qquad (6)$$

Dispersions of Correlated Objects.[17−19] If the positions of the objects in the dispersion are not completely random, the interferences between rays scattered by neighboring objects do not cancel out, and the intensity is modified by these interferences. For concentrated dispersions of identical, spherical objects, the intensity can be expressed as

$$I(Q) = NI_1(Q)S(Q) \qquad (7)$$

where $I_1(Q)$ is the intensity of noncorrelated objects and $S(Q)$ is the structure factor that describes the correlations. $S(Q)$ is a Fourier transform of the pair correlation function of the dispersion. For repelling objects, such as surfactant micelles, $S(Q)$ is depressed at low Q because long wavelength fluctuations of the number density of micelles are suppressed by the repulsions; it has a peak at a Q value corresponding to the most probable intermicellar distance d ($Q = 2\pi/d$), and it oscillates back to unity at higher Q values.

The scattering from micelles has been extensively studied; from the shape of the peak in the intensity, it is possible to calculate the parameters that determine the structure of the micellar solution, i.e. the micelle size, shape, and the strength of intermicellar repulsions.

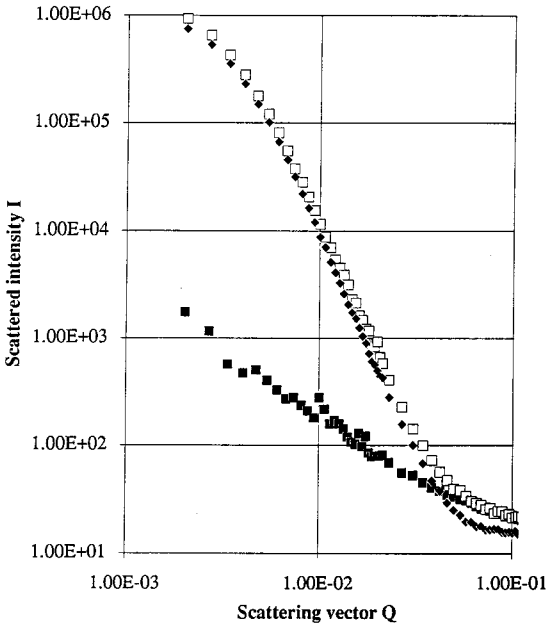

Figure 6. Scattering curves from pure semidilute EHEC solutions (concentration 0.5%) at different temperatures: (filled squares) 20 °C; (open squares) 40 °C; (filled diamonds) 60 °C. The slow rise of intensity toward $Q \rightarrow 0$ in the 20 °C data reflects a weak association of the dissolved macromolecules. The steep rise and very high intensities in the 40 and 60 °C data reflect macroscopic separation into domains of a polymer-rich phase and excess aqueous phase.

Instruments. Scattering experiments were performed on the instrument PACE of LLB, in Saclay. Neutrons of 11 or 20 Å wavelengths were focused on the sample through a 5 m collimator tube with 10 mm circular holes at both ends. With a sample to detector distance of 4.75 m, the accessible range of Q values was 0.002−0.02 Å^{-1}. With a sample to detector distance of 2.5 m, the accessible range of Q values was 0.01−0.1 Å^{-1}. The scattered neutrons were collected according to the scattering angle by an array of 30 circular detectors. The data were then normalized for the area and efficiency of detector cells. Subsequently, background spectra were subtracted from sample spectra, and spectra obtained at different detector positions were grouped in a single file. Finally, spectra corresponding to different polymer or surfactant concentrations were compared. It was found that the high-Q limit of the spectra was simply proportional to the surfactant concentration, as expected from the calculation of contrasts (see above). Thus, spectra corresponding to the same TeBo concentration and different EHEC contents merged together at high Q.

Scattering from Pure EHEC Solutions

Samples of EHEC in D_2O have been examined through SANS at two concentrations, both in the semidilute regime (0.5% and 3%), and three temperatures: 20, 40, and 60 °C.

At the lowest temperature, the samples are transparent, fluid solutions. The scattering is weak, and it decays slowly with Q (Figure 6). The scattering curves obtained at both concentrations are quite similar. Starting from the high-Q end of the scattering curve, which corresponds to the shortest distances, one finds a Q^{-1} law, which corresponds to scattering by rodlike objects. This was expected, since the EHEC macromolecules are semirigid and therefore must appear rodlike

at short distances. At lower Q values (below 0.01 Å^{-1}), corresponding to larger distances (beyond 100 Å), the scattering rises more steeply (Q^{-2}) toward the $Q \rightarrow 0$ limit. This is surprising, since in this range of distances the scattering should be controlled by interferences between macromolecules. Indeed, the average distance between EHEC "rods" in a 0.5% solution is 43 Å; at larger distances, the solution should appear homogeneous. Therefore the scattering curves should saturate instead of rising at low Q. Therefore the solution contains some macroscopic objects which cause the excess scattering at low Q. This scattering may be caused by incomplete dissociation, or weak association of the EHEC macromolecules.

At the higher temperatures the samples are white, indicating *phase separation*. The intensity scattered at low Q is quite large, and it has a marked curvature (Figure 6). At intermediate Q values, it decays as Q^{-4}. Accordingly, the scattering is produced by large globular objects; these must be *domains, or lumps, of the polymer-rich phase* which separates at these temperatures (see Figure 2). The very high intensities (3 orders of magnitude higher than that at 20 °C) indicate that these domains have collected most of the EHEC in the sample. It is remarkable that these domains are of a finite size. A plot of the low-Q intensity according to the Guinier law, eq 3, gives radii in excess of 1000 Å in the more concentrated sample (3%) and still larger in the more dilute one (0.5%). Thus, both samples appear unable to achieve a complete separation of the lumps formed by the polymer-rich phase.

Scattering from EHEC + TeBo

In these mixed systems, we observe the spatial distribution of surfactant molecules together with side groups of EHEC. At 20 °C, where the samples are clear solutions, the scattering shows mostly micelles; at 40 or 60 °C, where the samples are gels, the scattering reveals a structure made of lumps, with a lump size that is determined by the EHEC/TeBo ratio (ratio of the EHEC and TeBo concentrations, used throughout the text).

Room Temperature: $T = 20$ °C. Starting from the pure EHEC solution (spectrum similar to that in Figure 6), the addition of surfactant produces a depression at low Q and a shoulder at $Q = 0.04$ Å^{-1} (Figure 7). At high surfactant concentration (EHEC/TeBo < 2), the shoulder turns into a peak; the location of this peak corresponds to the average intermicellar distance (160 Å) if it is assumed that the surfactant forms regular micelles. Similarly, starting from the pure micellar solution, the addition of polymer leaves the intermicellar peak unchanged at $Q = 0.04$ Å^{-1} and produces a rise at small Q which tends toward that of the pure EHEC solution (Figure 8).

Thus, at low amounts of surfactant, the macromolecules remain weakly associated (low-Q rise of the intensity), and the surfactant forms micelles which may be bound to the polymer. At high amounts of surfactant, the micelles are distributed as they are in the pure surfactant solution (peak at 0.04 Å^{-1}), and the macromolecules are dissociated (the excess scattering at low Q has been depressed).

Intermediate Temperature: $T = 40$ °C. We have seen that the pure EHEC + water system at 40 °C gives a very large intensity at low Q, caused by lumps of the polymer-rich phase (see Figure 6). The *addition of surfactant* depresses the low-Q intensity and reduces the downward curvature of the scattering curve (Figure

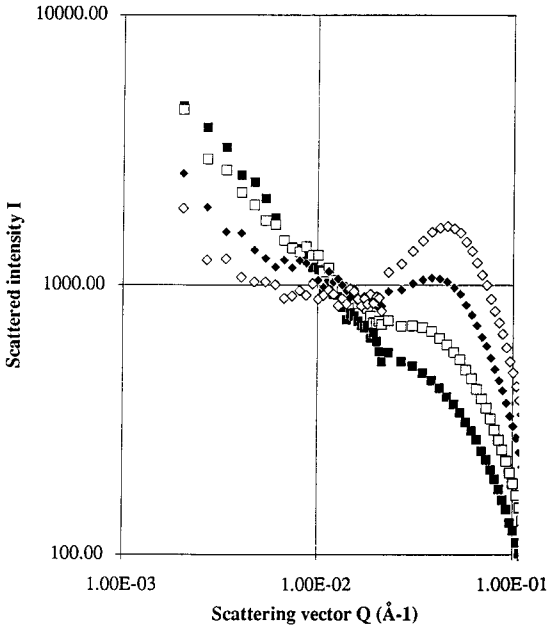

Figure 7. Samples with a fixed EHEC concentration (1.5%) and variable TeBo content, at 20 °C: (open diamonds) TeBo 1.5%; (filled diamonds) TeBo 0.9%; (open squares) TeBo 0.5%; (filled squares) TeBo 0.3%. The peak observed at high Q in the samples with excess surfactant is caused by TeBo micelles. All these samples were clear fluid solutions at 20 °C.

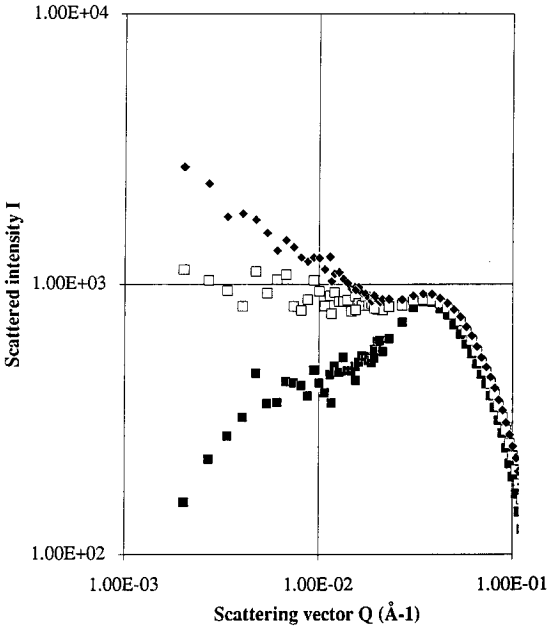

Figure 8. Samples with a fixed TeBo concentration (0.72%) and variable EHEC content, at 20 °C: (filled diamonds) EHEC 1.5%; (open squares) EHEC 0.6%; (filled squares) no EHEC. The peak observed at high Q in the samples with excess surfactant is caused by TeBo micelles. All these samples were clear fluid solutions at 20 °C.

9). According to eqs 2 and 3, the reduced curvature indicates a *decrease in the sizes of lumps*. At higher surfactant concentrations (EHEC/TeBo < 2), the low-Q intensity drops rapidly, and a peak appears at high Q (Figure 10). The peak position corresponds to the average intermicellar distance if it is assumed that most of the surfactant forms excess micelles.

Conversely, starting from the pure micellar solution, the addition of EHEC first produces a slight shift in the intermicellar peak, and then a fast rise of the intensity at low Q when the ratio EHEC/TeBo exceeds 2 (Figure 11). *There is a range of compositions where the lumps,*

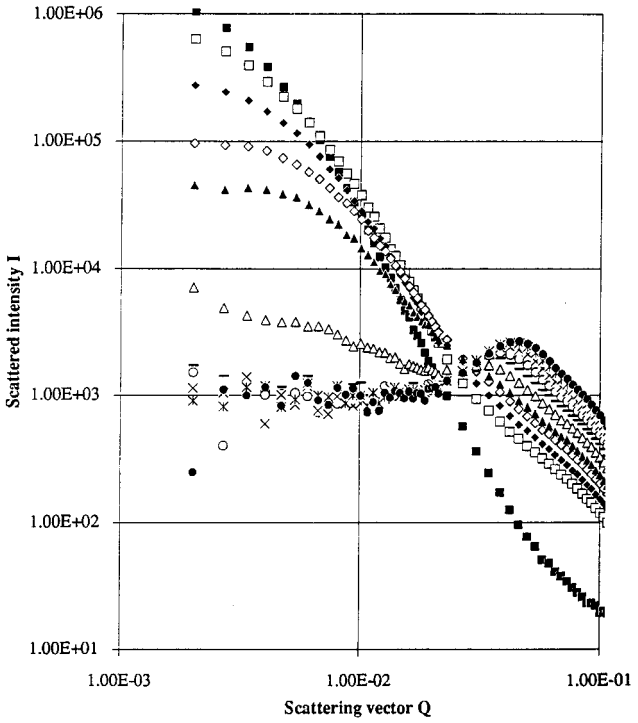

Figure 9. Samples with a fixed EHEC concentration (1.5%) and variable TeBo content, at 40 °C. Starting with the curve that is the highest at low *Q*, the concentrations of TeBo are 0 (phase separated), 0.3%, 0.4%, 0.5%, 0.6% (all turbid, decreasing turbidity); 0.9% (clear gel); and 1.2%, 1.5%, 1.8%, 2.1%, 2.4% (clear solutions with decreasing viscosity).

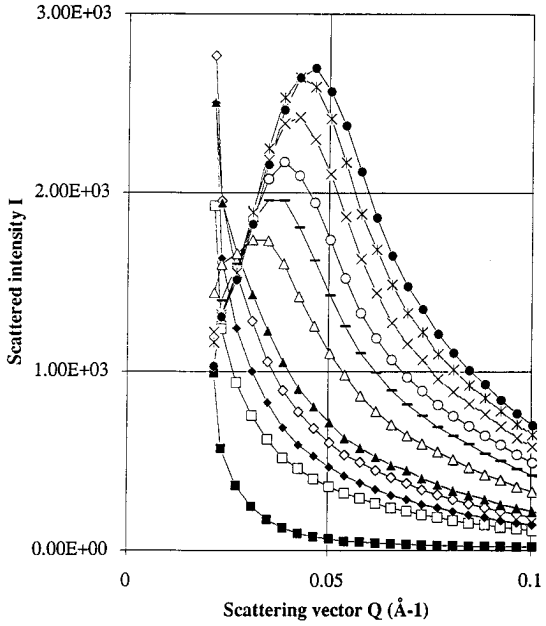

Figure 10. Enlargement of the data presented in Figure 9, in the region of the intermicellar peak, and in linear scales. The highest intensities at the peak are from samples with higher TeBo concentrations.

which cause the low-Q scattering, coexist with excess micelles, which cause the peak at high Q. The coexistence is observed at EHEC/TeBo values ranging between 1.6 and 2.5. The rise of one signal with the decrease of the other looks like two-phase behavior.

At higher EHEC concentrations (EHEC/TeBo > 2.5), the intermicellar peak vanishes completely, and the scattering is caused by the lumps only. As the spectra cover 2 decades in *Q* values and 3−4 decades in intensity, it is possible to make meaningful fits with the

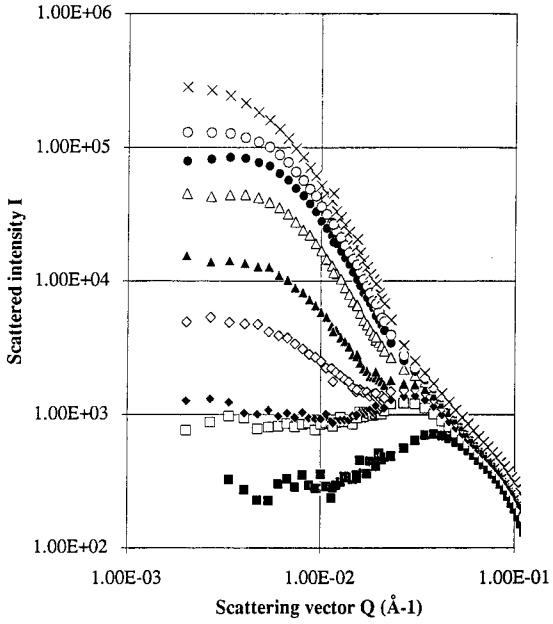

Figure 11. Samples with a fixed TeBo concentration (0.72%) and variable EHEC content, at 40 °C. Starting with the curve that is the highest at low *Q*, the concentrations of EHEC are 3%, 2.4%, 2.1%, 1.8% (all of them clouded gels); 1.5% (clear gel, filled triangles); 1.2% (clear viscous solution); and 0.9%, 0.6%, 0 (clear fluid solutions).

calculated scattering curves of simple objects. Some of these fits are presented in the next three figures.

The calculated curves must reproduce three features of the experimental spectra: the initial curvature, which reflects the outer radii of the objects, the slope in the intermediate *Q* range, and the asymptotic slope at high *Q*. In most cases, both slopes are Q^{-2}; in some cases, the intermediate slope is Q^{-4} (as for homogeneous spheres) and the asymptotic slope is Q^{-2} (as for shells). A complete series of fits was made for the samples at fixed TeBo concentrations and variable amounts of EHEC. Starting with excess surfactant, the first spectra show the coexistence of lumps (at low *Q*) with excess micelles (shoulder at high *Q*); this is presented in Figure 12 for the composition EHEC 1.5%, TeBo 0.72%. When the EHEC/TeBo ratio exceeds 2, the low-*Q* scattering rises, the scattering from excess micelles vanishes, and the whole spectrum is fitted by the calculated scattering curve for polydisperse spherical shells. This is presented in Figure 13 for the composition EHEC 3%, TeBo 0.72%. Since the scattering is contributed mainly by the surfactant, *the match with a scattering curve of shells implies that the surfactant is located on the surfaces of the lumps.*

A similar trend is observed with fixed EHEC concentration and decreasing amounts of TeBo. Excess micelles are observed at high TeBo, and they vanish at EHEC/TeBo = 3. At lower amounts of surfactant, the whole scattering curve is fitted by the calculated curve for shells. This is presented in Figure 14 for the composition EHEC 1.5%, TeBo 0.5%. Accordingly, the surfactant must be located on the surfaces of lumps that have this characteristic size. At the lowest surfactant concentrations (EHEC 1.5%, TeBo 0.3%) the scattering curve is below that of shells and closer to that of homogeneous spheres. In this case, the surfactant concentration is so low that the scattering from the polymer becomes significant; consequently, the scattering curve reflects the interior of the lumps (containing polymer) more than their surface (where the surfactant is located).

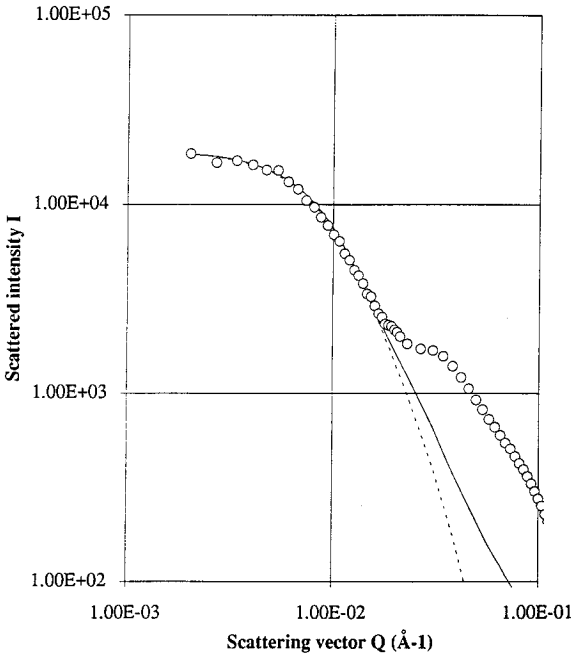

Figure 12. Fit of the scattering curve of a sample containing 1.5% EHEC and 0.72% TeBo, at 40 °C, with the calculated scattering curves for polydisperse spheres (dotted line) and shells (continuous line). The mean radius of the shells is 170 Å. The shoulder at high *Q* is from excess micelles.

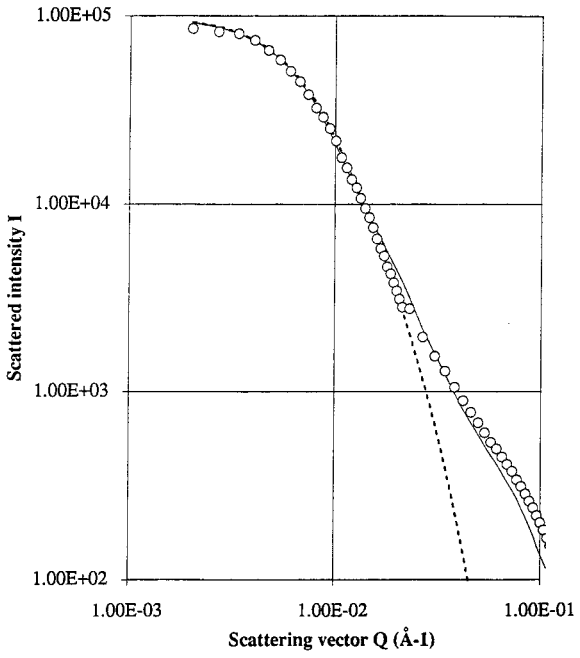

Figure 14. Fit of the scattering curve of a sample containing 1.5% EHEC and 0.5% TeBo, at 40 °C, with the calculated scattering curves for a set of shells (full line) or spheres (dotted line). The mean outer radius of the shells is 230 Å, and the mean outer radius of the spheres is 300 Å.

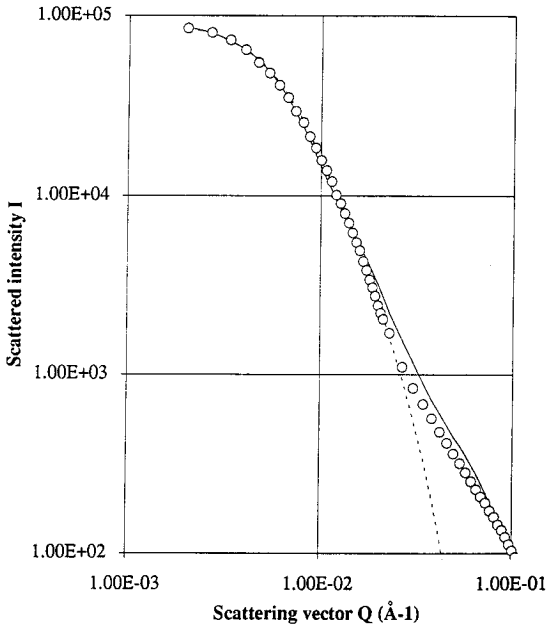

Figure 13. Fit of the scattering curve of a sample containing 3% EHEC and 0.72% TeBo, at 40 °C, with the calculated scattering curves for a set of shells (full line) or spheres (dotted line). The mean outer radius of the shells is 260 Å, and the mean inner radius is 10% smaller; the distribution of radii is triangular, and it extends from 30% of the mean to 170% of the mean. The fit with shells indicates that the surfactant is located at the surfaces of the lumps formed by the polymer-rich phase.

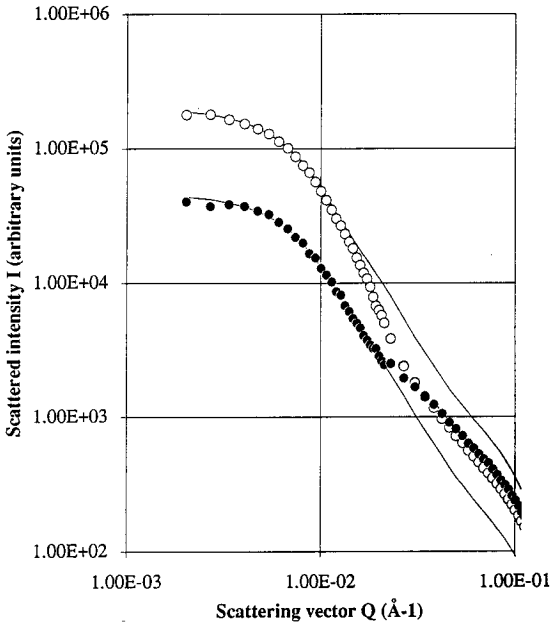

Figure 15. Comparison of the scattering curves measured at 40 °C (dots) and 60 °C (circles) for a sample containing 1.5% EHEC and 0.6% TeBo. The fits are made with the calculated curves for a set of shells. The mean radii are respectively 200 and 210 Å. The higher intensities measured at 60 °C in the low-*Q* part of the scattering curve reflect the increase in content of the lumps.

High Temperature: *T* = 60 °C. The spectra obtained at 60 °C are generally similar to those obtained at 40 °C, but the changes in the scattering curves with the EHEC/TeBo ratio are more abrupt than those shown in Figures 9 and 11, and they occur at a lower EHEC/TeBo ratio. A comparison of individual scattering curves is presented in Figure 15 for the composition EHEC 1.5%, TeBo 0.6%. At very low *Q*, where the intensity measures the content of the lumps that cause scattering, it is 4 times higher for the measurement at 60 °C. At higher *Q*, the radii extracted from the curvature of the scattering curves at both temperatures are the same. At still higher *Q*, the decay of the 60 °C curve has the steep slope of homogeneous spheres, while the 40 °C curve has the weaker decay of hollow shells. Finally, at the high-*Q* limit, where the scattering originates from the interfaces, both curves merge.

These features may be interpreted in terms of the phase separation of EHEC. At 60 °C, the contrast between the polymer-rich phase that forms the interior of the lumps and the external phase that separates the

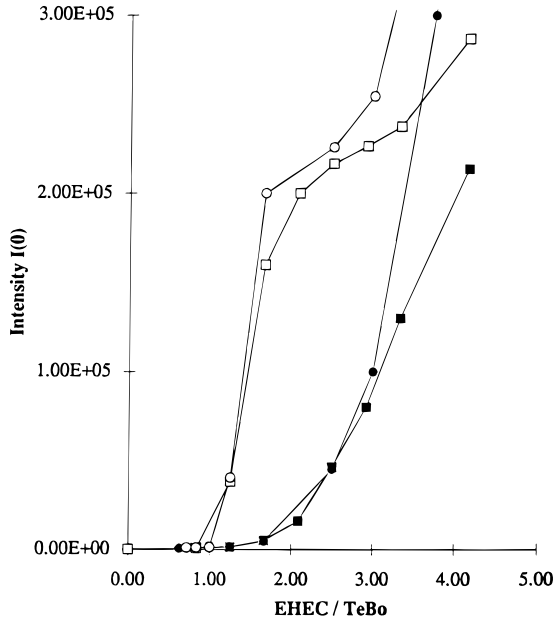

Figure 16. Values of the low-Q limit of the intensity, according to the EHEC/TeBo ratio. These values reflect the surfactant content per lump of the polymer-rich phase. Filled symbols: values measured at 40 °C for the variable TeBo series (dots) and the variable EHEC series (squares). Open symbols: values measured at 60 °C for the variable TeBo series (circles) and the variable EHEC series (squares).

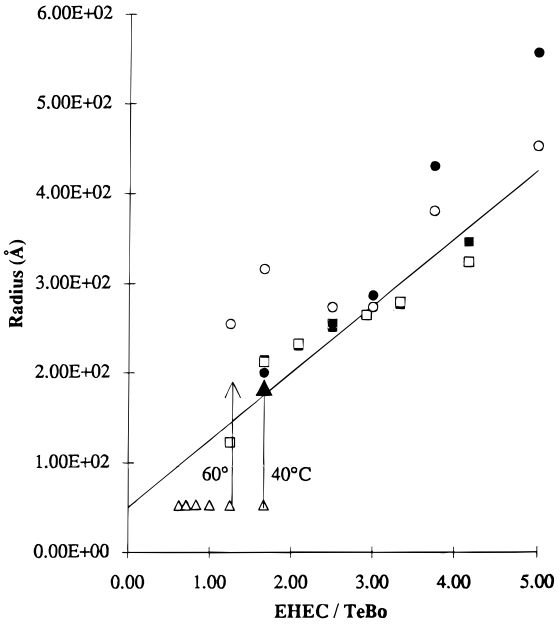

Figure 17. Radii of the lumps formed by the polymer-rich phase, according to the EHEC/TeBo ratio. Filled symbols: values measured at 40 °C for the variable TeBo series (dots) and the variable EHEC series (squares). Open symbols: values measured at 60 °C for the variable TeBo series (circles) and the variable EHEC series (squares). Open triangles: sizes of the excess micelles, according to the value of the average intermicellar distance. The straight line fit corresponds to the theoretical law for a distribution of the surfactant as a dense monolayer at the surfaces of fully dense polymer lumps.

lumps is high and controls the scattering, hence the higher intensities and the scattering curve that resembles that of homogeneous spheres. At 40 °C, just above the onset of turbidity, this contrast is low, and the scattering is caused by the surfactant only, hence the weaker intensities and the scattering curve that resembles that of shells.

All the results concerning the lumpy structure of the mixed systems can be summarized by the values of the intensity at $Q \rightarrow 0$ and of its curvature at low Q. The values of $I(Q \rightarrow 0)$ give the average content per lump; they are presented in Figure 16 for both temperatures. The 40 °C intensities rise progressively when the EHEC/TeBo ratio is increased above 1.6; this is consistent with the fact that the objects seen by scattering do not have a dense interior (they resemble shells or objects of low dimensionality). The 60 °C intensities show an abrupt rise at EHEC/TeBo = 1.2, and saturate at higher values; this is consistent with the fact that the objects seen by scattering have a dense interior (they resemble homogeneous spheres). It is instructive to compare these values with the visual turbidity of the samples: samples that gave intensies below 50 000 in the arbitrary units used here were transparent to the eye; in samples that gave intensities between 50 000 and 200 000, the eye could detect some turbidity; higher intensities came from samples that were white and opaque.

The radii of the lumps were extracted from the fits; they are presented in Figure 17 for both temperatures. At low values of EHEC/TeBo, only the intermicellar peak is seen, and the corresponding micellar radius is indicated. There is a transition region where micelles and lumps coexist, as mentioned above. Beyond this transition, we measured the radii of lumps, which start at 160 Å and increase continuously with the ratio EHEC/TeBo. Both series of samples and both temperatures gave similar radii; the rise with EHEC/TeBo appears to be linear. It is also instructive to compare these results with the flow properties of the samples: *all samples that contained micelles only were fluid; all samples that contained lumps were gels.*

Discussion

The central feature of EHEC + surfactant systems is the transition that occurs as the temperature is raised. Visual observation shows dramatic changes in the appearance of the samples (turbidity, viscosity) as the phase transition is approached from below. Structural data presented above also show dramatic changes, such as the formation of a lumpy structure at the expense of the micellar organization, again as the transition is approached from below. However it is difficult to analyze this behavior in a quantitative rather than qualitative way because the effects of temperature on the association are hard to quantify.

For this reason we chose to use composition as the main variable, crossing the transition in two ways: adding surfactant to modify the phase separation of EHEC, or adding EHEC to the pure surfactant solution. Comparing these two sets of experiments at the same values of the EHEC/TeBo ratio, we obtained identical results. For instance, the radii and intensities measured in both sets at the same value of EHEC/TeBo are the same (Figures 16 and 17).

The variation of structure according to the EHEC/TeBo ratio can be observed directly on the scattering curves: as shown in Figures 9 and 11, the addition of surfactant causes a transfer of intensity from small Q values to high Q values. Accordingly, *the structure, initially phase separated on a large scale, becomes more homogeneous.* Quantitative data are provided by the measured radii and intensities: initially, the samples contain domains of the polymer-rich phase which are much larger than 1000 Å; upon addition of surfactant the sizes of these lumps are reduced all the way to 160 Å, and their content varies accordingly. Thus, *the effect*

of surfactant is to fragment the domains of the polymer-rich phase into microscopic lumps.

Examination of the scattering curves at 40 °C reveals that the surfactant is collected into large aggregates with low dimensionality, such as shells or porous objects. This is consistent with the idea that the surfactant causes fragmentation of large domains of the polymer-rich phase into microscopic lumps and therefore ends up at the surfaces of these lumps. Fits of the scattering curves with the calculated curves of shells give radii which vary linearly with the EHEC/TeBo ratio (Figure 17). This simple law must have its origin in the relative locations of EHEC and TeBo. This is easily demonstrated if it is assumed that the polymer-rich phase is fragmented into spherical lumps covered with surfactant monolayers. Let R be the radius of a lump, C_p the concentration of the polymer-rich phase inside the lumps, ΔR the thickness of the surfactant monolayer, and C_s the concentration of surfactant in this layer. Then the amount of available surfactant determines the total surface area of the lumps, and therefore their size, according to

$$R = 3\Delta R(V/\Delta V) = 3\Delta R(\text{EHEC/TeBo})(C_s/C_p) \quad (8)$$

This behavior may result from the fact that *the surfactant is adsorbed on the lumps of the polymer-rich phase;* it is not unique to the spherical geometry. For instance, if the lumps of the polymer-rich phase were actually fibers covered with surfactant, then the law would be

$$R = 2\Delta R(V/\Delta V) = 2\Delta R(\text{EHEC/TeBo})(C_s/C_p) \quad (9)$$

Moreover, it is not necessary for the surfactant to form continuous monolayers at the surfaces of the lumps. In fact, considering that the polymer-rich phase still contains a substantial amount of water, it could be that the surfactant forms small aggregates bound to the more hydrophobic nodes of the polymer phase, at the locations where dissociation took place. This grainy structure of the surfactant would still give the same scattering curves, provided that the surfactant aggregates are quite small and located on a two-dimensional surface.

At higher surfactant contents, the lumps vanish abruptly and micelles are formed. This transition looks like the solubilization of emulsion droplets by micelles. The boundaries of the transition region are determined by the minimal sizes below which the lumps become unstable and by the amount of polymer that can be solubilized by the micelles. The behavior of the scattering across this transition looks like two-phase behavior; however, no macroscopic phases can be separated at this transition.

If the insoluble material were made of small molecules such as polar oils, this emulsification model would be completely adequate. In this case, the stable state of the system at low surfactant concentration would be the macroscopic phase separation of oil from the micellar phase, and the emulsion would be a metastable state. However, the lump structure that forms the gels appears to be a stable state of the system: it forms either upon heating, from the homogeneous micellar solution, or upon cooling, when a polymer-rich phase that has expelled water and surfactant swells again to form these finite lumps. Therefore, the polymeric nature of the poorly soluble material and its heterogeneous chemical structure must be important. In this respect, the behavior of these polymer + surfactant systems is closer to a *microphase separation*.[20,21]

At this point we have enough structural information to understand the origin of this thermoreversible gelation. The critical information is provided by the comparison of structures with mechanical properties. On the one hand, all samples that contained micelles only were fluid. Therefore the associations of micelles with the macromolecules must have a short lifetime.[22] On the other hand, all samples that contained the microscopic lumps were gels. Therefore the lumps provide permanent connectivity to the system. This feature must originate from the fact that many macromolecules are needed to form a lump, whereas the number of macromolecules associated to a micelle is of the order of unity.

Conclusion

The original aim of this work was to understand the relation between (a) the thermoreversible gelation of mixed EHEC + surfactant systems and (b) the phase behavior of pure EHEC solutions, which separate into a polymer-rich phase and an excess aqueous phase. The answer to this question is that the addition of surfactant transforms a macroscopic phase separation into a microphase separation. The microphase-separated state is made of lumps of the polymer-rich state that are kept apart from each other by the adsorption of surfactant. These lumps provide the connectivity of the system, while the space between them retains all the water that would have been expelled in the absence of surfactant. This combination of swelling and connectivity matches the definition of a gel.

Acknowledgment. We thank Ingegerd Lind for skillful technical assistance, Akzo-Nobel for supplying the polymer and the surfactant, and the Swedish Research Council for Engineering Sciences (TFR) for partial financial support.

References and Notes

(1) Annable, B.; Buscall, R.; Ettelaie, R.; Whittlestone, D. *J. Rheol.* **1993**, *37*, 695.
(2) Annable, B.; Buscall, R.; Ettelaie, R.; Shepherd, P.; Whittlestone, D. *Langmuir* **1994**, *10*, 1060.
(3) Leibler, L. *Macromolecules* **1990**, *13*, 1602.
(4) Goddard, E. D. *Colloids Surf.* **1986**, *19*, 255 and 301.
(5) Cabane, B. *J. Phys. Chem.* **1977**, *81*, 1639.
(6) Cabane, B.; Duplessix, R. *J. Phys. (Fr.)* **1982**, *43*, 1529.
(7) Cabane, B.; Duplessix, R. *Colloids Surf.* **1985**, *13*, 19.
(8) Cabane, B.; Duplessix, R. *J. Phys. (Fr.)* **1987**, *48*, 651.
(9) Piculell, L.; Lindman, B. *Adv. Colloid Interface Sci.* **1992**, *41*, 149.
(10) Carlsson, A.; Karlström, G.; Lindman, B. *Colloids Surf.* **1990**, *47*, 147.
(11) Carlsson, A. Doctoral thesis, University of Lund, Sweden, 1989.
(12) Lindell, K.; Engström, S. *Int. J. Pharm.* **1993**, *95*, 219.
(13) Lindell, K.; Engström, S. *Int. J. Pharm.* **1995**, *124*, 107.
(14) Carlsson, A.; Karlström, G.; Lindman, B. *Langmuir* **1986**, *2*, 536.
(15) Jacrot, B. *Rep. Prog. Phys.* **1976**, *39*, 911.
(16) Cabane, B. In *Surfactants in Solution: New Methods of Investigation*; Zana, R., Ed.; Dekker: New York, 1986.
(17) Hayter, J. B.; Penfold, J. *J. Chem. Soc., Faraday Trans. 1* **1981**, *77*, 1851.
(18) Hayter, J. B.; Penfold, J. *Mol. Phys.* **1981**, *42*, 109.
(19) Cabane, B.; Duplessix, R.; Zemb, T. *J. Phys. (Fr.)* **1985**, *46* 2161.
(20) Khlokhlov, A. R.; Nyrkova, I. A. *Macromolecules* **1992**, *25*, 1493.
(21) Nyrkova, I. A.; Khlokhlov, A. R. *Macromolecules* **1993**, *26*, 3601.
(22) Nyström, B.; Thuresson, K.; Lindman, B. *Langmuir* **1995**, *11*, 1994.

MA951526K